scientific reports

Check for updates

OPEN

Competitive adsorption behavior and adsorption mechanism of limestone and activated carbon in polymetallic acid mine water treatment

Chang Yin, Yongbo Zhang✉, Yongjiang Tao & Xueping Zhu

Acid mine water (AMD) can cause significant environmental hazards due to its high concentration of metal ions, so the development of effective treatment methods is essential to mitigate its impact. In this study, adsorption experiments were conducted using limestone (LS) and activated carbon (AC) to explore the adsorption efficiency for different concentrations of metal ions. Adsorption was evaluated by static and competitive batch tests. The adsorbent mechanism was investigated using analytical techniques such as SEM, FTIR and XRD. The efficacy of LS and AC for competitive adsorption of Fe, Mn, Zn and Cu ions from AMD was evaluated. The study analyzed the effect of environmental conditions such as initial concentration and ionic strength on the adsorption efficiency. The results showed that LS showed high adsorption capacity for Fe and Cu, but was less effective in competitive adsorption of Mn. AC showed superior adsorption performance for Fe and Cu under competitive conditions due to its high surface area and functional groups. Both adsorbents showed selective efficacy influenced by the physicochemical properties of metal ions. This study helps to guide the optimization of adsorbents in AMD treatment and highlights the importance of selecting suitable materials based on specific metal ion properties.

Keywords Acid mine drainage, Adsorbents, Adsorption characteristic, Wastewater

Water is the source of human existence[1], however, with the development of industry, industrial processes such as metal plating, battery manufacturing, mining operations, etc. generate large quantities of polluted water containing high concentrations of heavy metal ions[2]. In particular, acid mine water (AMD) is one of the main sources of this highly concentrated polluted water[3]. Acid mine water is produced by the interaction of pyrite with water and air in mining areas[4]. It contains high concentrations of acids and heavy metal ions, and when high concentrations of heavy metal ions such as copper, zinc, and iron in AMD exceed the permissible limits, it can have a destructive effect on the ecosystem, pollute the condition of the local water resources, and threaten the survival and development of human beings[5,6]. In particular, it causes acute toxicity to aquatic plants and animals, inhibits growth, promotes lipid peroxidation and DNA damage[7].

Commonly used AMD remediation technologies are categorized into active and passive treatment technologies, and the economically viable industrial technologies available today are precipitation, adsorption, electrochemical processes, and membrane processes treatment[8–10]. Among these methods, adsorption is considered to be an effective and economical treatment method with flexibility in design and operation and a wide range of sources; agricultural wastes, industrial by-products, and natural substances can be used as adsorbents for heavy metal wastewater[11].Adsorbents are mainly categorized into natural and synthetic adsorbents. Natural adsorbents, such as plant wastes and natural inorganic materials, can effectively remove harmful dyes from wastewater[12,13].Synthetic adsorbents are materials prepared by synthetic methods for use in the adsorption process[14]. These materials usually have specific physicochemical properties that allow them to effectively adsorb and remove pollutants from water, such as heavy metal ions, organic compounds, dyes and other harmful substances[15].

In recent years, more studies have been conducted on synthetic adsorbents, which have the advantages of high adsorption efficiency, simple synthesis and wide range of applications[16]. The Nevertheless, synthetic adsorbents

Taiyuan University of Technology, Taiyuan 030024, China. ✉email: zhangyongbo2021@sina.com

are mostly prepared in the laboratory, using expensive equipment for complex preparation procedures, which may hinder large-scale applications, they are less stable, with large differences in performance, and face problems such as economic costs, energy consumption, and secondary pollution[17].

LS and AC are natural adsorbents[15,18], they are economical and convenient for the treatment of metal ions in AMD[11,18,19]. LS surface has a porous structure, which can make pollutants attach to the surface of LS through physical adsorption, and can also undergo ion exchange reaction with metals in solution, effectively absorbing metal ions such as Fe, Mn, etc. in wastewater[18,20–22]. Due to its porous structure and high specific surface area[23], various functional groups on the surface of AC, such as carboxyl, hydroxyl, and phenolic groups, can react chemically with pollutant molecules in water and form chemical bonds, which can effectively recover ferrous, manganese, and zinc ions from AMD[24–26].

Since AMD contains a variety of highly concentrated metal ions, the adsorption of metal ions from AMD by LS and AC is equivalent to the adsorption in a competing system[27]. In a competitive system, contaminants compete for limited adsorption sites, affecting the removal efficiency of metals[28]. Antagonistic and synergistic adsorption effects are exhibited between different ions. Lee et al. through the use of alginate beads and goethite alginate beads, they were found to effectively adsorb As(III) and As(V) from acidic mine drainage sludge[29,30].L et al. used silica membranes, which performed well in reducing the metal content in AMD[30,31]. Sandri Tandi Rapang et al. used physically and chemically activated eggshell AC for adsorption of iron and manganese from AMD[31]. Previous studies have focused on the adsorption of metal ions in AMD by different adsorbents[32,33],they did not explore the adsorption performance of adsorbents in competing systems for metal ions in AMD. Therefore, we used LS and AC as adsorbent materials to explore the differences in competitive adsorption of metal ions Fe, Zn^{2+}, Mn^{2+}, and Cu^{2+} in adsorbents, applied isothermal adsorption model and adsorption kinetic analysis, and applied SEM, FTIR, and XRD tests to deeply analyze the adsorption mechanism of LS and AC for adsorption of pollutants in acidic mine water.

Materials and methods

Materials

The experimental water samples were taken according to the acidic mine water in Niangziguan spring area of Shanxi Province as a reference, and the experimental water containing a certain concentration of pollutants was configured according to the experimental requirements. The pH value of the water samples was adjusted to 2.0, and the typical pollutant composition of acid mine water was shown in Table 1.

Two adsorption materials were used in this study: LS and AC. The specific sources and pretreatment methods for each material are listed below:

LS: High-calcium LS is selected and screened by mechanical crushing and passing through a 0.2 mm sieve. The screened limestone is dried at room temperature and stored in sealed containers for subsequent use.

AC: Spherical AC is used. The AC is first crushed in a pulverizer and subsequently sieved through a 0.2 mm sieve to ensure consistent particle size. After crushing and sieving, the AC is also dried at room temperature and stored under dry conditions.

Adsorbent characterization

Scanning electron microscopy (SEM) was used to examine the surface morphology and distribution of LS and AC before and after adsorption of metal ions. The spectra were recorded using a Fourier transform infrared spectrometer (FTIR). X-ray diffraction (XRD) was used to determine the bulk phase of the materials of LS and AC before and after adsorption.

Experiments

Metal ion static adsorption experiments

LS and AC were each added to the solution containing different concentrations of metal ions at a solid-liquid ratio of 100 g/L. The adsorption was carried out in a constant temperature oven. The experiments were carried out in a constant temperature chamber with the rotational speed set at 180 r/min and the adsorption time was 6 h. At the end of the experiment, the solids and liquids were separated by centrifugation and the concentration of metal ions in the supernatant was determined by UV atomic absorption. The experiment was set up with three sets of parallel samples.

Competitive adsorption experiments

Competitive adsorption experiments were performed using a mixed solution containing four metal ions (Fe^{2+}, Zn^{2+}, Mn^{2+}, Cu^{2+}) at concentrations of 10, 20, 30, 40, and 50 mg/L. The experimental procedure was the same as that of static adsorption experiments.

The water samples used for the experiments were manually configured. Different concentrations of metal ion solutions (Fe^{2+}, Zn^{2+}, Mn^{2+}, Cu^{2+}) were mixed in predetermined proportions and the pH was adjusted to about 4.0.

Ion	Mn^{2+}	Zn^{2+}	Cu^{2+}	Fe^{2+}
Content (mg/L)	18	10	4	50

Table 1. Acid mine drainage configuration table.

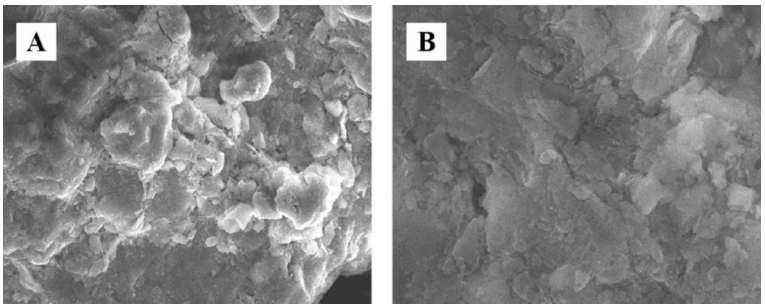

Fig. 1. SEM images of LS (A) and AC (B).

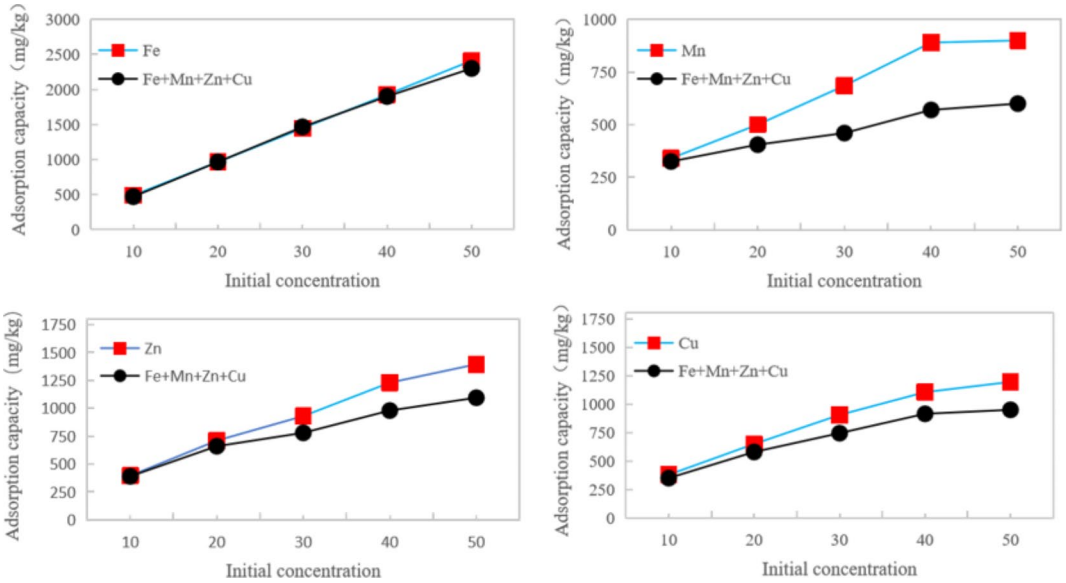

Fig. 2. Adsorption of Fe^{2+}, Mn^{2+}, Zn^{2+}, Cu^{2+} by LS and AC in single and competitive systems.

A single metal ion static adsorption experiment was used as a control, and the amount of adsorption was calculated by difference subtraction method, i.e., the difference between the metal ion concentration before and after adsorption. The experimental results were analyzed by taking the average of three sets of parallel samples.

Results and discussion

Analysis of SEM

The morphology and microstructure of LS and AC were observed by SEM (Fig. 1). It shows that there are differences in the morphology of LS and AC. LS has a large pore structure with a rough, irregular and uneven surface distribution (Fig. 1A). AC has smaller voids, fine surface and uniform distribution (Fig. 1B).

Analysis of single versus competing systems

The effect of LS and AC on the adsorption of metal ions was studied according to the initial concentration (Figs. 2 and 3). In a single system, the adsorption of all tested ions by LS showed an increasing trend with increasing initial concentration. For Fe^{2+} and Zn^{2+}, the adsorption capacity of LS continued to increase with increasing initial concentration, indicating that the adsorption of these two ions had not reached saturation. For Mn^{2+} and Cu^{2+}, the adsorption curves tended to stabilize with the increase of initial concentration, indicating that the adsorption of these two ions by LS was gradually saturated. The adsorption capacity of AC for Fe^{2+}, Cu^{2+} and Zn^{2+} showed a significant increasing trend, which is in accordance with the results of ALOthman et al.[34], while the increase in adsorption of Mn^{2+} was relatively slow, indicating the limited adsorption capacity of AC for Mn^{2+}.

In the competitive system, the adsorption curves of LS for all four metal ions showed a downward shift, reflecting that when multiple metal ions coexisted, the inter-ionic competition would lead to a decrease in the adsorption amount of each ion. Among them, Mn showed the most significant decrease in adsorption, indicating that Mn was not a preferred ion to be adsorbed by LS in the competitive adsorption process. In contrast, the decrease in the adsorption amount of Fe^{2+} was smaller, indicating that the other three ions had less influence on its adsorption. The adsorption amounts of AC for all four metal ions decreased, especially for the other three

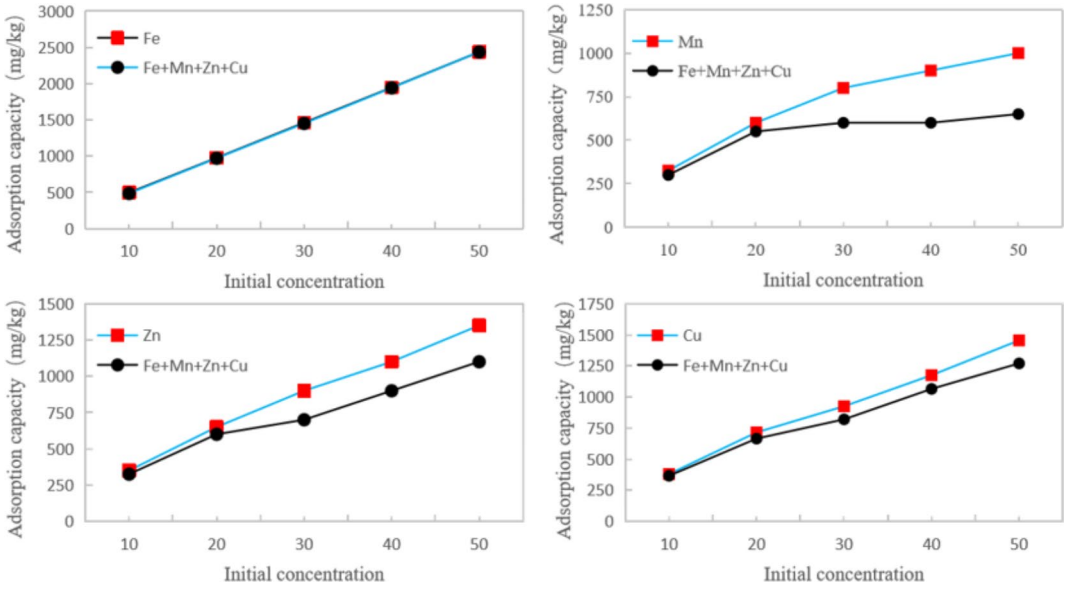

Fig. 3. Adsorption of Fe^{2+}, Mn^{2+}, Zn^{2+}, Cu^{2+} by AC in single and competitive systems.

ions except Fe^{2+}. This phenomenon suggests that ions other than Fe^{2+} are more inhibited in the competition for adsorption sites with AC under the conditions of coexistence of multi-metal ions. The smaller decrease in the adsorption amount of Fe^{2+} suggests that Fe^{2+} has some advantages in the competitive adsorption.

Enrichment coefficient analysis

In order to gain a deeper understanding of the competitive adsorption characteristics of LS with AC metal ions, the Enrichment Coefficient (E) was introduced as an evaluation index in this study (Equation S1).

$$E = C_{sample}/C_{solution} \times 100\% \quad \text{(S1)}$$

C_{sample} is the amount of metal ions adsorbed in the sample (mg/kg). $C_{solution}$ is the ionic amount of the metal before adsorption (mg/kg)

The enrichment coefficients of LS for the four metal ions showed a gradual decrease with the increase of the initial concentration, both in the single system and in the competitive system (Table 2). In the competitive system, compared with the single system, the adsorption of four ions by LS was affected to different degrees, and the enrichment coefficients were all reduced. Especially for Mn, the enrichment factor decreased the most, indicating that the adsorption capacity of LS on Mn was significantly inhibited during the competitive adsorption process. While Fe showed the smallest decrease in enrichment coefficient, indicating that Fe was more advantageous in competitive adsorption[35]. The strongest adsorption capacity of LS in competitive adsorption was for Fe^{2+}, and the weakest for Mn^{2+}, followed by Zn^{2+} and Cu^{2+}.

Under a single system, AC exhibited high enrichment factors for all metal ions tested, whereas these enrichment factors generally decreased under the competitive system, reflecting the interaction between metal ions in competitive adsorption (Table 3). In particular, Mn showed the largest decrease in enrichment factor, indicating that it was most significantly affected in competitive adsorption, while Fe^{2+} showed a relatively small decrease in enrichment factor. This result further confirms that Fe^{2+} has relatively strong competition for the adsorption sites of AC, while Mn^{2+} has weak competition for the adsorption sites of AC in the environment of coexisting polymetallic ions.

Adsorption kinetic analysis

During the adsorption process, different metal ions interact with each other in the polymetallic ion system, where kinetic fitting is the most dominant approach[36].

Dynamics analysis of data using pseudo-first-order dynamics models(PFO) and pseudo-second-order dynamics models(PSO)[37,38].The fitted curves and parameters of LS and AC for the adsorption of metal ions are shown in Fig. 4; Table 4. The correlation coefficients of the pseudo-second-order kinetic model of LS (R) are larger than those of the pseudo-first-order kinetics and the theoretical values of the pseudo-second-order model are the same as the experimental values. Therefore, the kinetics of metal ion adsorption on LS can be accurately described by the pseudo-second-order model.

In AC, the correlation coefficients of the pseudo-first-order kinetic model for iron ions were larger than those of the pseudo-second-order kinetic model, and the correlation coefficients of the adsorption of manganese, zinc, and copper ions by AC were larger for the pseudo-second-order kinetic model than for the pseudo-first-order kinetic model (Fig. 5). The results indicate that the adsorption process is controlled by chemisorption, which is the same as the results of Duan, Chen et al.[39,40].

	Zn^{2+}			Cu^{2+}			Fe^{2+}			Mn^{2+}		
Concentration (mg/L)	Unitary	Competitiveness	Decrease (%)	Unitary	Competitiveness	Decrease (%)	Unitary	Competitiveness	Decrease (%)	Unitary	Competitiveness	Decrease (%)
10.0	79.8	78.8	1.0	76.8	70.8	5.9	96.0	94.0	2.0	68.0	65.0	3.0
20.0	70.3	65.3	5.0	64.4	57.4	6.9	97.5	96.5	1.0	50.0	40.5	9.5
30.0	63.8	52.7	10.0	61.1	50.3	10.8	98.0	97.7	0.3	45.7	30.7	15.0
40.0	63.7	50.8	13.0	57.3	47.4	9.8	97.3	95.0	2.3	44.5	28.5	16.0
50.0	57.1	44.8	12.3	48.8	28.8	10.0	96.0	92.0	4.0	36.0	24.0	12.0

Table 2. Enrichment coefficients of LS for four metal ions.

Concentration (mg/L)	Zn^{2+}			Cu^{2+}			Fe^{2+}			Mn^{2+}		
	Unitary	Competitiveness	Decrease (%)	Unitary	Competitiveness	Decrease (%)	Unitary	Competitiveness	Decrease (%)	Unitary	Competitiveness	Decrease (%)
10.0	70.0	65.0	5.0	76.8	73.9	2.8	99.0	97.0	2.0	65.0	60.0	1.0
20.0	65.0	60.0	5.0	70.8	65.8	4.9	97.5	97.0	0.5	60.0	55.0	5.0
30.0	60.0	46.7	13.3	62.5	55.4	7.1	97.3	97.1	0.2	53.0	40.0	13.0
40.0	55.5	45.0	10.0	60.8	55.2	5.6	97.3	97.0	0.3	45.0	30.0	15.0
50.0	54.0	44.0	10.0	59.5	51.9	7.6	97.4	97.4	0.0	40.0	14.0	14.0

Table 3. Enrichment coefficients of AC for four metal ions.

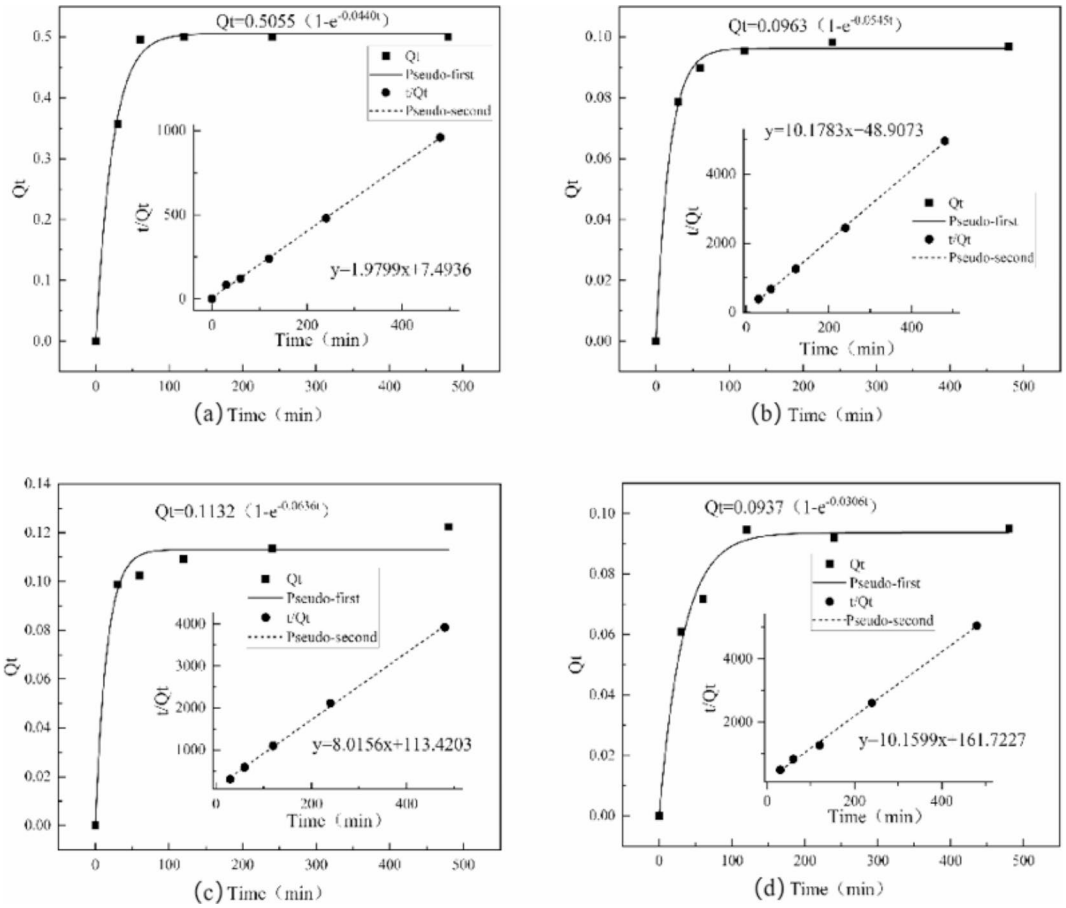

Fig. 4. Model of adsorption kinetics of metal ions on LS.

Solute	Adsorbent	Model	a	b	R^2
Fe^{2+}	LS	PFO	0.5055	0.04397	0.994
		PSO	7.4936	1.9799	0.999
	AC	PFO	0.4522	0.0138	0.995
		PSO	1.9796	0.0322	0.990
Mn^{2+}	LS	PFO	0.1132	0.0636	0.979
		PSO	113.4203	8.0156	0.998
	AC	PFO	0.1132	0.0636	0.979
		PSO	113.42	8.0516	0.998
Zn^{2+}	LS	PFO	0.0936	0.0306	0.983
		PSO	161.7227	10.1599	0.9987
	AC	PFO	0.0819	0.0112	0.977
		PSO	887.4621	9.8556	0.994
Cu^{2+}	LS	PFO	0.09625	0.05451	0.998
		PSO	48.9073	10.1783	0.999
	AC	PFO	0.03864	0.02487	0.998
		PSO	594.2216	23.9318	0.999

Table 4. The parameters of LS and AC for the adsorption of metal ions.

Activation energy

The activation energy (Ea) is the energy required to overcome the energy barrier in the adsorption process. Higher activation energies imply that the adsorption process is more selective and chemisorption dominates, while lower activation energies indicate that physical adsorption plays a major role.

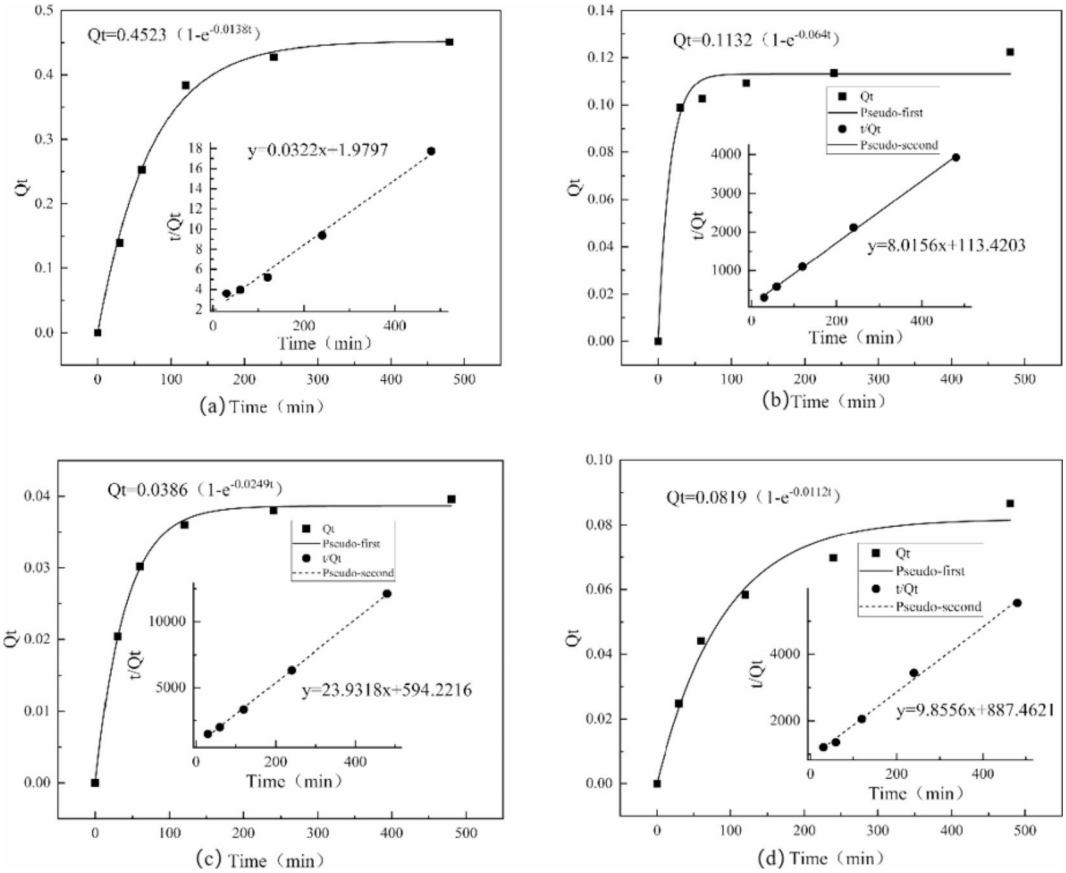

Fig. 5. Model of adsorption kinetics of metal ions on AC.

Solute	Adsorbent	K_L (L/mg)	Q_m (mg/g)	R^2
Fe^{2+}	LS	1.01	5.747	0.954
	AC	2.83	4.41	0.921
Mn^{2+}	LS	0.805	1.887	0.904
	AC	0.166	2.871	0.996
Zn^{2+}	LS	0.162	3.184	0.997
	AC	0.069	4.081	0.972
Cu^{2+}	LS	0.159	2.786	0.969
	AC	0.112	3.676	0.988

Table 5. Langmuir adsorption model fitting parameters.

The Ea for the adsorption process of each metal ion on LS and AC was calculated using the Arrhenius equation (Equation S4). The following Ea is obtained: Fe^{2+}: 18.52 kJ/mol, Mn^{2+}: 10.12 kJ/mol, Zn^{2+}: 5.35 kJ/mol, and Cu^{2+}: 7.41 kJ/mol. These values indicate that Fe^{2+} adsorption requires the highest energy, suggesting a more complex chemical interaction with both adsorbents. In contrast, Zn^{2+} and Mn^{2+}, with lower activation energies, are more easily adsorbed via physical processes. The moderate activation energy of Cu^{2+} suggests a combination of physical and chemical adsorption, which aligns with its observed high adsorption efficiency on AC.

Effects of adsorption isotherms

The isotherm data were further analyzed by Langmuir Isotherm (Equation S2) and Freundlich (Equation S3) to investigate the surface properties of LS and AC[41]. As shown in Tables 5 and 6, for LS, Langmuir curves were better fitted for Fe^{2+}, Zn^{2+} with maximum adsorption of 5.747 mg/g and 3.184 mg/g, respectively. Freundlich was able to better fit Mn^{2+} and Cu^{2+} with maximum adsorption of 1.887 mg/g and 2.786 mg/g, respectively.

For AC, Freundlich fits well for Fe^{2+}, Mn^{2+} and Zn^{2+} with maximum adsorption of 4.41 mg/g, 2.871 mg/g and 4.081 mg/g, respectively, and for Cu^{2+}, both Langmuir and Freundlich fit well with a maximum adsorption of 3.676 mg/g. Thus, LS adsorbs better for Fe^{2+}. AC has better adsorption of Mn^{2+} and Zn^{2+}.

Solute	Adsorbent	K_F (ml/mg)	n	R^2
Fe^{2+}	LS	3.127	1.01	0.676
	AC	3.561	1.684	0.937
Mn^{2+}	LS	0.387	2.913	0.950
	AC	0.371	1.931	0.947
Zn^{2+}	LS	0.537	1.851	0.985
	AC	0.353	1.550	0.996
Cu^{2+}	LS	0.501	1.976	0.979
	AC	0.466	1.664	0.988

Table 6. Freundlich adsorption model fitting parameters.

Adsorption heat

- The heat of adsorption represents the energy released or absorbed during adsorption and is often used to distinguish between physical[42] and chemical adsorption. For chemical adsorption, the heat of adsorption is large, usually 40–400 kJ/mol[43], whereas the heat of adsorption is lower for physical adsorption. The heat of adsorption can be estimated from the relationship between Langmuir's constant (K_L) and temperature (Equation S5). The adsorption heat of the four metal ions is shown in Table 7.
- The adsorption heat (ΔH) for the adsorption of Fe^{2+}, Mn^{2+}, Zn^{2+}, and Cu^{2+} on LS and AC supports the observation that both materials exhibit selective adsorption behavior. The relatively low ΔH values indicate that the process is primarily governed by physical adsorption. For example, Fe^{2+} showed the lowest adsorption heat on both LS (-0.25 kJ/mol) and AC (-2.92 kJ/mol), consistent with its stronger adsorption affinity in the competitive environment.

Adsorption mechanism of LS and AC

The surface functionality of adsorbents plays a crucial role in the adsorption of metal ions. Functional groups such as hydroxyl (-OH), carboxyl (-COOH), and phenolic groups on the surface of AC and LS are key factors in determining their adsorption behavior. These groups can form chemical bonds with metal ions, participate in ion exchange reactions, or facilitate electrostatic interactions, thereby enhancing the adsorption efficiency.

SEM was used to study the shape and structure of the surfaces in LS and AC (Fig. 6)[44]. Compared to before adsorption (Fig. 1), after adsorption, it was evident that the inter-particle voids in LS and AC were effectively filled (Fig. 6A), and the surfaces were relatively filled flat and smooth, indicating that the pollutants in acid mine water were effectively adsorbed[45].

X-ray diffraction (XRD) was used to study the plots of LS and AC before and after reaction with four metal ions. As shown in Fig. 7. the main components of LS before adsorption are calcium carbonate and calcium oxide. Before and after adsorption, the intensity of the diffraction peaks obviously changed, and the diffraction peaks of calcium carbonate increased, which may be due to the fact that Ca in the LS reacted with SO_4^{2-} in the mine water to produce a slightly water-soluble precipitate, which increased the solution pH and led to the removal of Fe^{2+}, Mn^{2+}, Zn^{2+} and Cu^{2+} by precipitation. Many new peaks appeared in many positions after adsorption on AC, and it was inferred that the corresponding complexes might have been generated on the surface of AC through electrostatic action and ion exchange.

FTIR spectroscopy was applied to identify the functional groups on LS and AC before and after the reaction, and the changes of the groups in the adsorbent were determined by observing the splitting, drifting, appearance and disappearance of the peaks in the plots, as shown in Fig. 8. Analyzing the infrared spectra before and after the adsorption of LS, (a) it can be obtained that the peaks' intensities changed in the range of 711.49–862.93 cm, which may be due to the lattice vibration of anionic SO caused a part of SO_4^{2-} adsorbed on the surface of LS. After the adsorption of AMD by LS, a fine sharp peak was formed in the range of 3500–3700 cm^{-1}, which indicated that LS chemisorbed heavy metal ions. Analyzing the infrared spectrograms before and after the adsorption of AC, it can be obtained that there are no obvious new peaks in (b), but there is an obvious

Solute	Adsorbent	ΔH (kJ/mol)
Fe^{2+}	LS	-0.25
	AC	-2.92
Mn^{2+}	LS	-1.94
	AC	-7.80
Zn^{2+}	LS	-7.89
	AC	-11.61
Cu^{2+}	LS	-8.00
	AC	-9.38

Table 7. The adsorption heat of the four metal ions.

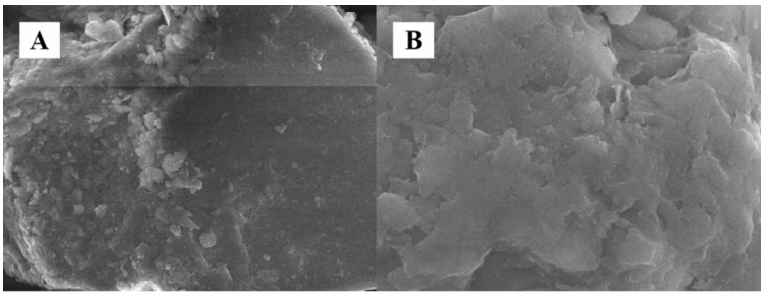

Fig. 6. SEM images of LS (A) and AC (B) after metal ion adsorption.

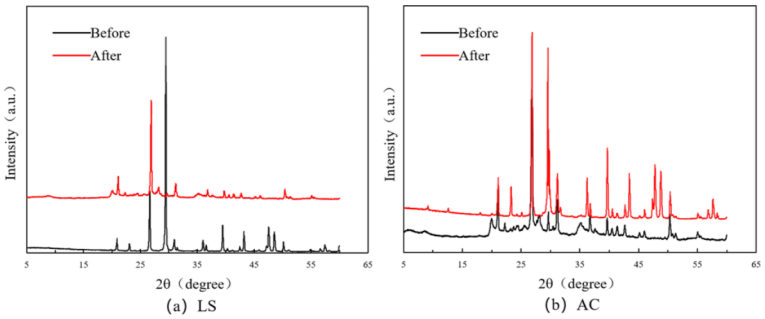

Fig. 7. XRD patterns of LS(a) and AC(b) before and after adsorption.

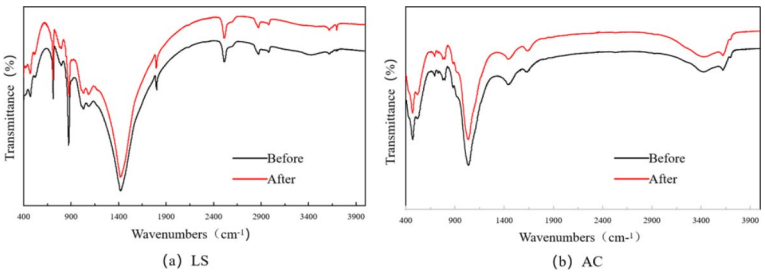

Fig. 8. FTIR spectra of LS(a) and AC(b) before and after adsorption.

vibrational peak shift phenomenon, and the intensity of some of the peaks has also changed. The reason may be that the functional groups such as -OH and -CO in AC complexed with heavy metal ions, resulting in the change of peaks. The adsorption heats for Zn^{2+} and Cu^{2+} on AC are higher compared to those on LS, indicating stronger interactions between these metal ions and the functional groups on AC's surface. This supports the hypothesis that AC's porous structure and surface chemistry enhance the chemisorption of these ions, especially Cu^{2+}, which exhibited the highest adsorption heat on AC (-9.38 kJ/mol). The calculated Ea provide insight into the adsorption mechanisms of LS and AC. The high activation energy for Fe^{2+} (18.52 kJ/mol) suggests strong chemical adsorption, likely due to the ion exchange reactions and complex formation between Fe^{2+} and the surface functional groups of the adsorbents. On the other hand, Mn^{2+} and Zn^{2+} exhibit lower activation energies (10.12 kJ/mol and 5.35 kJ/mol, respectively), indicating that their adsorption is predominantly governed by physical processes, such as electrostatic interactions. The intermediate activation energy for Cu^{2+} (7.41 kJ/mol) supports a mixed adsorption mechanism, where both physical and chemical interactions contribute to its high adsorption efficiency.

Conclusion

- In this study, the competitive adsorption of Fe^{2+}, Mn^{2+}, Zn^{2+}, and Cu^{2+} by LS and AC was investigated. LS showed the highest adsorption efficiency for Fe^{2+}, while AC excelled in Cu^{2+} and Fe^{2+} adsorption. The coexistence of multiple ions resulted in competitive adsorption, with Mn^{2+} often being suppressed. Electronegativity, hydration energy, and physicochemical properties of the adsorbents were key factors influencing adsorption. Adsorption heats and activation energies suggest that physical adsorption dominates for Mn^{2+}

and Zn^{2+}, while Fe^{2+} exhibits stronger chemical interactions with LS and AC. The findings highlight the role of adsorbent properties and environmental conditions, especially pH, in determining adsorption efficiency. These results provide valuable insights for applying LS and AC in industrial wastewater treatment, particularly in managing AMD. This offers a cost-effective and sustainable solution for industries facing challenges in the management of heavy metal pollution, ensuring both compliance with environmental regulations and the protection of aquatic ecosystems. Future work should explore the long-term stability of adsorbents and investigate surface modifications to enhance chemisorption and improve selectivity in competitive systems. Advancing analytical techniques like XPS or Raman spectroscopy could offer deeper insights into adsorption mechanisms and guide material optimization.

Data availability

Data is available on request from Chang Yin (yinchang327@163.com).

Received: 7 August 2024; Accepted: 24 September 2024
Published online: 09 October 2024

References

1. S, G. D. Water in the evolution of human civilization - the origin of life. *Int. Res. J. Tamil.* **4**, 18–23 (2022).
2. Azimi, A., Azari, A., Rezakazemi, M. & Ansarpour, M. Removal of heavy metals from industrial wastewaters: A review. *Chembioeng. Rev.* **4**, 37–59 (2017).
3. Vareda, J. P., Valente, A. J. M. & Durães, L. Assessment of heavy metal pollution from anthropogenic activities and remediation strategies: A review. *J. Environ. Manage.* **246**, 101–118 (2019).
4. Singer, P. C. & Stumm, W. Acidic mine drainage: The rate-determining step. *Science* **167**, 1121–1123 (1970).
5. Simate, G. S. & Ndlovu, S. Acid mine drainage: Challenges and opportunities. *J. Environ. Chem. Eng.* **2**, 1785–1803 (2014).
6. Vardhan, K. H., Kumar, P. S. & Panda, R. C. A review on heavy metal pollution, toxicity and remedial measures: Current trends and future perspectives. *J. Mol. Liq.* **290**, 111197 (2019).
7. Radić, S., Vujčić, V., Cvetković, Cvjetko, P. & Oreščanin, V. The efficiency of combined cao/electrochemical treatment in removal of acid mine drainage induced toxicity and genotoxicity. *Sci. Total Environ.* **466–467**, 84–89 (2014).
8. Jacobs, J. A. Overview of soil and groundwater sampling methods for acid drainage Studies. 119–122. (2014).
9. Naidu, G. et al. A critical review on remediation, reuse, and resource recovery from acid mine drainage. *Environ. Pollut.* **247**, 1110–1124 (2019).
10. Rodríguez-Galán, M. et al. Remediation of acid mine drainage. *Environ. Chem. Lett.* **17**, 1529–1538 (2019).
11. Fu, F. & Wang, Q. Removal of heavy metal ions from wastewaters: A review. *J. Environ. Manag.* **92**, 407–418 (2011).
12. Dąbrowski, A. Adsorption—from theory to practice. *Adv. Colloid Interface Sci.* **93**, 135–224 (2001).
13. Sharma, P., Kaur, H., Sharma, M. & Sahore, V. A. Review on applicability of naturally available adsorbents for the removal of hazardous dyes from aqueous waste. *Environ. Monit. Assess.* **183**, 151–195 (2011).
14. Momin, Z. H., Angaru, G. K. R., Lingamdinne, L. P., Koduru, J. R. & Chang, Y. Highly efficient cd(II) removal from groundwater utilizing layered mixed metal oxides-graphitic carbon nitride composite with improved cycling stability. *J. Water Process. Eng.* **56**, 104276 (2023).
15. Tran, V. S. et al. Typical low cost biosorbents for adsorptive removal of specific organic pollutants from water. *Bioresour. Technol.* **182**, 353–363 (2015).
16. Jafari, Z., Avargani, V. M., Rahimi, M. R. & Mosleh, S. Magnetic nanoparticles-embedded nitrogen-doped carbon nanotube/porous carbon hybrid derived from a metal-organic framework as a highly efficient adsorbent for selective removal of pb(II) ions from aqueous solution. *J. Mol. Liq* **318**, 113987 (2020).
17. Han, B., Butterly, C., Zhang, W., He, J. & Chen, D. Adsorbent materials for ammonium and ammonia removal: A review. *J. Clean. Prod.* **283**, 124611 (2021).
18. Sdiri, A. & Bouaziz, S. Re-evaluation of several heavy metals removal by natural limestones. *Front. Chem. Sci. Eng.* **8**, 418–432 (2014).
19. Ziemkiewicz, P. F., Skousen, J. G., Brant, D. L., Sterner, P. L. & Lovett, R. J. Acid mine drainage treatment with armored limestone in open limestone channels. *J. Environ. Qual.* **26**, 1017–1024 (1997).
20. Watten, B. J., Sibrell, P. L. & Schwartz, M. F. Acid neutralization within limestone sand reactors receiving coal mine drainage. *Environ. Pollut.* **137**, 295–304 (2005).
21. Iakovleva, E. et al. Acid Mine Drainage (Amd) treatment: neutralization and toxic elements removal with unmodified and modified limestone. *Ecol. Eng.* **81**, 30–40 (2015).
22. Silva, D., Weber, C. & Oliveira, C. Neutralization and uptake of pollutant cations from acid mine drainage (Amd) using limestones and zeolites in a pilot-scale passive treatment system. *Min. Eng.* **170**, 107000 (2021).
23. Momin, Z. H. et al. Redefining water purification: Gc3N4-Cldh's electrochemical Smx eradication. *Chemosphere* **362**, 142921 (2024).
24. Mohan, D. & Chander, S. Single component and multi-component adsorption of metal ions by activated carbons. *Colloids Surf. A* **177**, 183–196 (2001).
25. Anirudhan, T. S. & Sreekumari, S. S. Adsorptive removal of heavy metal ions from industrial effluents using activated carbon derived from waste coconut buttons. *J. Environ. Sci.* **23**, 1989–1998 (2011).
26. Kumar, N., Pandey, A. & Sharma, Y. C. A review on sustainable mesoporous activated carbon as adsorbent for efficient removal of hazardous dyes from industrial wastewater. *J. Water Process. Eng.* **54**, 104054 (2023).
27. He, S. et al. Competitive adsorption of Cd2+, Pb2 + and Ni2 + onto Fe3+-modified argillaceous limestone: influence of Ph, ionic strength and natural organic matters. *Sci. Total Environ.* **637–638**, 69–78 (2018).
28. Gabaldón, C., Marzal, P., Ferrer, J. & Seco, A. Single and competitive adsorption of Cd and Zn onto a granular activated carbon. *Water Res.* **30**, 3050–3060 (1996).
29. Lee, H. et al. As(III) and as(V) removal from the aqueous phase via adsorption onto acid mine drainage sludge (Amds) alginate beads and goethite alginate beads. *J. Hazard. Mater.* **292**, 146–154 (2015).
30. Trisnaliani, L., Purnamasari, I. & Ahmadan, F. Performance of silica membranes from fly ash coal of Pt semen baturaja in reducing metal content in mine acid water. *Indones. J. Fundam. Appl. Chem.* (2019).
31. Rapang, S. T. et al. Decrease levels of Iron (Fe) and manganese (mn) in acid mining water using active carbon of egg shell. *J. Chem.* (2022).
32. Moreroa-Monyelo, M., Falayi, T., Ntuli, F. & Magwa, N. Studies towards the adsorption of sulphate ions from acid mine drainage by modified attapulgite clays. *S. Afr. J. Chem. Eng.* **42**, 241–254 (2022).
33. Restiawaty, E., Gozali, V. A., Wibisono, T. A. S. E. & Budhi, Y. W. Utilizing modified clinoptilolite for the adsorption of heavy metal ions in acid mine drainage. *Case Stud. Chem. Environ. Eng.* **9**, 100706 (2024).

34. ALOthman, Z. A. et al. Adsorptive removal of Cu(II) and pb(II) onto mixed-waste activated Carbon: Kinetic, thermodynamic, and competitive studies and application to real wastewater samples. *Arab. J. Geosci.* **9**, (2016).
35. Noda, K., Uchida, S. & Miyazaki, M. Limestone neutralization of acid solutions containing dissolved iron. *J. Chem. Eng. Jpn.* **22**, 253–257 (1989).
36. Zhou, W., Wu, H. & Yildirim, T. Enhanced H2 adsorption in isostructural metal – organic frameworks with open metal sites: Strong dependence of the binding strength on metal ions. *J. Am. Chem. Soc.* **130**, 15268–15269 (2008).
37. Saiers, J. E., Hornberger, G. M. & Liang, L. First- and second-order kinetics approaches for modeling the transport of colloidal particles in porous media. *Water Resour. Res.* **30**, 2499–2506 (1994).
38. Momin, Z. H. et al. Exploring recyclable alginate-enhanced gcn-ldo sponge for U(VI) and cd(II) removal: Insights from batch and column studies. *J. Hazard. Mater.* **469**, 134015 (2024).
39. Duan, J. & Su, B. Removal characteristics of cd(II) from acidic aqueous solution by modified steel-making slag. *Chem. Eng. J.* **246**, 160–167 (2014).
40. Chen, W. et al. New insights into adsorption of as(V) and sb(V) from aqueous by Hco–(Fe3O4)X adsorbent: Adsorption behaviors, competition and mechanisms. *J. Water Process. Eng.* **58**, 104873 (2024).
41. Aguayo-Villarreal, I. A., Bonilla-Petriciolet, A. & Muñiz-Valencia, R. Preparation of activated carbons from Pecan Nutshell and their application in the antagonistic adsorption of Heavy Metal ions. *J. Mol. Liq.* **230**, 686–695 (2017).
42. Dormant, L. M. & Adamson, A. W. Physical adsorption behavior of molecular solids. *J. Colloid Interface Sci.* **28**, 459–465 (1968).
43. Singh, N. & Campbell, C. T. A Simple Bond-Additivity Model Explains Large Decreases in Heats of Adsorption in Solvents Versus Gas Phase: A Case Study with Phenol On Pt(111) in Water. *Acs Catal.* **9**, 8116–8127 (2019).
44. Momin, Z. H., Ahmed, A. T. A., Malkhede, D. D. & Koduru, J. R. Synthesis of thin-film composite of mwcnts-polythiophene-Ru/Pd at liquid-liquid interface for supercapacitor application. *Inorg. Chem. Commun.* **149**, 110434 (2023).
45. Momin, Z. H. et al. Improving U(VI) retention efficiency and cycling stability of GCN-supported calcined-LDH composite: Mechanism insight and real water system applications. *Chemosphere* **346**, 140551 (2024).

Author contributions

Yin Writing original draft, review & editingZhang Conceptualization Funding acquisitionZhu SupervisionTao Data curationAll authors reviewed the manuscript.

Declarations

Competing interests

The authors declare no competing interests.

Additional information

Supplementary Information The online version contains supplementary material available at https://doi.org/10.1038/s41598-024-74240-8.

Correspondence and requests for materials should be addressed to Y.Z.

Reprints and permissions information is available at www.nature.com/reprints.

Publisher's note Springer Nature remains neutral with regard to jurisdictional claims in published maps and institutional affiliations.